Optimizations and artificial neural network validation studies for naphthalene and phenanthrene adsorption onto NH_2-UiO-66(Zr) metal-organic framework

Z U Zango[1,2,*], K Jumbri[1,3,*], H F M Zaid[4], N S Sambudi[4], J Matmin[5]
[1]Fundamental and Applied Sciences Department, Universiti Teknologi PETRONAS, 32610 Seri Iskandar, Perak, Malaysia.
[2]Department of Chemistry, Al-Qalam University Katsina, P.M.B 2137, Katsina, Nigeria.
[3]Centre of Research in Ionic Liquids (CORIL), Institute of Contaminant Management, Universiti Teknologi PETRONAS, 32610 Seri Iskandar, Perak, Malaysia
[4]Chemical Engineering Department, Universiti Teknologi PETRONAS, 32610 Seri Iskandar, Perak, Malaysia.
[5]Department of Chemistry, Faculty of Science, Universiti Teknologi Malaysia, 81310 UTM Johor Bahru, Johor, Malaysia
*Corresponding author: zakariyya4@gmail.com, khairulazahar.jumbri@utp.edu.my

Abstract. Adsorptive removal of naphthalene (NAP) and phenanthrene (PHE) was reported using NH_2-UiO-66(Zr) metal-organic frameworks. The process was optimized by response surface methodology (RSM) using central composite design (CCD). The fitting of the model was described by the analysis of variance (ANOVA) with significant Fischer test (F-value) of 85.46 and 30.56 for NAP and PHE, respectively. Validation of the adsorption process was performed by artificial neural network (ANN), achieving good prediction performance at node 6 for both NAP and PHE with good agreement between the actual and predicted ANN adsorption efficiencies. The good reusability of the MOF was discovered for 7 consecutive cycles and achieving adsorption efficiency of 89.1 and 87.2% for the NAP and PHE, respectively. The performance of the MOF in a binary adsorption system was also analyzed and the adsorption efficiency achieved was 97.7 and 96.9% for the NAP and PHE, respectively.

1. Introduction

Water contamination due to polycyclic aromatic hydrocarbons (PAHs) has been a recurring phenomenon due to the excessive use of petroleum and petrochemical products. They are usually released from petroleum and allied industries in form of wastewater effluents into the environment where they cause significant damage in the receiving environment waters [1]. Concentrations of PAHs is also significantly increased due to the frequent oil spills in the sea and oceans as a result of petroleum transportations, combustion of oil from the ships and leakage of the oil tankers [2]. Owing to their stabilities and hydrophobic nature, PAHs drastically threatens the life of aquatic organisms and affect the human health [3, 4]. Naphthalene and phenanthrene are among the 16 PAHs categorized as priority organic pollutants by the United State Environmental Protection Agency (USEPA) and European Environmental Agency (EEA) [5, 6]. They have high mobility and long-term persistency in water due to their lower solubility.

They are practically non-degradable by photolysis and natural sunlight due to their aromatic nature. Biological treatment has been widely employed as wastewater purification technology due to its cost effectiveness, however some PAHs are known to be less biodegradable, and some inhibited the biological process [7], hence the process is ineffective for their remediations [8]. Similarly, the conventional coagulation method is not sufficient for the removals. Conventional activated sludge system has also been reported for the treatment of petrochemical plants wastewaters, incomplete removal of the PAHs was resulted [9]. Thus, the desire to explore other wastewater remediation methods for their effective treatments. Despite the existence of various wastewater remediation process, adsorption was considered ideal technology for the removal of most organic pollutants due to its low-cost, less energy demand, broad spectrum of adsorbents from both natural and synthetic origins, and the fact that the spent adsorbent can be regenerated and reused [10]. Thus, various adsorbents such as activated carbon have been used for the PAHs removal from wastewater [11]. Recently, the use of advanced porous materials such as metal-organic frameworks have gained recognition in wastewater remediations [12]. Of the most widely employed are the zirconium (Zr) [13, 14] and iron (Fe) [15, 16] based MOFs due to their extensive surface area and porosity as well as high hydrothermal stabilities.

Artificial neural network (ANNs) is a form of machine learning widely employed for making predictions and validation of findings from simulations, statistical modeling, and experimental analysis [17]. It is a developed machine learning tool capable of understanding rather complicated functions of non-linear statistical data and processed the output with high precision. It was developed to mimic the functions of the human brain by accepting sets of data and process the information to arrive at a certain conclusion [18]. Thus, it has been widely used in science and engineering to validate experimental design and improve the precision of the data, optimized the experimental conditions, and make predictions on the experimental findings [19, 20]. The process capitalizes on the experimental data to extract the information from the parameters of operation and make generalization for the whole process.

Thus, the aim of this work is to study the adsorption of NAP and PHE onto NH2-UiO-66(Zr) MOF. The adsorption was optimized by response surface methodology RSM according to the central composite design (CCD) quadratic model. ANN will be employed to validate the experimental findings and predicts the adsorption efficiency of the MOF.

2. Materials and Methods

All the chemicals used in this study were analytical grade and used as received. The PAHs standards: Naphthalene (99% purity) and Phenanthrene (98% purity), Zirconium tetrachloride (99.99% purity), Amino terephthalic acid (97% purity) were purchased from Sigma Aldrich (USA). Other solvents such as dimethyl formamide and ethanol were supplied by Avantis Laboratory, Malaysia.

2.1. Synthesis and characterization of the MOFs

The synthesis of NH_2-UiO-66(Zr) was achieved by solvothermal method, and the detail of the procedure was described in our previously studies.

2.2. Preparation of the stock solution

The synthesis of NH2-UiO-66(Zr) was achieved by solvothermal method, and the detail of the procedure was described in our previously studies.

2.3. Synthesis and characterization of the MOFs

The acenaphthene stock solution was prepared in acetone by using 10 mg of the standard in 100 ml volumetric flask to make a solution of 100 mg/L. Working solution was prepared from the stock solution in double deionized water using serial dilutions.

2.4. Adsorption study

Batch adsorption experiment was designed by the RSM software (Design Expert 11) using full factorial CCD comprises of 5 input variables: contact time (min), dosage (mg), concentration (mg/L), pH and

temperature (°C) with 5 center points. The adsorption was conducted using 30 mL of the NAP and PHE and phenanthrene solution in an incubator shaker (Incubator ES 20/60, bioSan) at 200 rpm. The sample was analyzed using UV-visible spectrophotometer (GENESYS 30) analysis at 276 and 250 nm for the NAP and PHE, respectively. The responses were determined as the percentage adsorption efficiency achieved by the NH_2-UiO-66(Zr) from the formula:

$$\%R = \frac{C_0 - C_e}{C_0} X\ 100 \quad (1)$$

And the amount of the acenaphthene adsorbed onto the MOFs at certain time (qt) and equilibrium (qe) were determine from the formula:

$$q_t = \frac{(C_0 - C_t)V}{w} \quad (2)$$

$$q_e = \frac{(C_0 - C_e)V}{w} \quad (3)$$

where C_0, C_t and C_e are the initial, time and equilibrium concentrations (mg/L), respectively, w is the weight of adsorbent (g), and V is the volume of the solution (L).

2.5. ANN modeling

ANN model was employed for the validation of the adsorption data developed from the RSM design based on the CCD according to the five inputs variables: the contact time, dosage, concentration, pH, and temperature. The overall data used was 282 which was divided into training (60%), testing (20%) and validation (20%). Thus, Multilayer perceptron ANN (MLP-ANN) was used with back-propagation algorithm and log-sigmoid activation function according to the multiple neurons from the input layers and the hidden layers to determine the output layers. Changing the weight of the hidden layer resulted in the best ANN architecture according to the fitting of the R^2 and RMSE [234].

2.6. Reusability and binary studies

The reusability experiment was carried out with PAHs solution of 4 mg/L solution and 5 mg of the adsorbent. After equilibrium was achieved, the MOFs was regenerated by dissolving the analytes in 50 mL of absolute ethanol for 1 h and then thoroughly washed with double distilled water and dried in vacuum for 5 hours at 100 °C. For binary adsorption, the removal of NAP and PHE was made under similar adsorption medium.

3. Results and discussions

The amino terephthalate MOF, NH_2-UiO-66(Zr) was successfully synthesized and characterized for the crystal structure, morphology, functional groups, and thermal stability as reported in our previous work [21]. It comprised of a milky powder with uniform particle size. The surface area and porosimetry analysis has revealed the porous nature of the MOF with BET and Langmuir surface area of 985 and 1445 m^2/g respectively. Thus, the promising features of the MOF for adsorptive removal of pollutants from water has been established. Thus, the experimental design for NAP and PHE adsorption onto the MOF was achieved using RSM software according to the CCD with 5 factors primary adsorption parameters: the contact time, dosage, concentration, pH, and temperature.

3.1. Model Statistical analysis

The fitting of the RSM quadratic model for the experimental data was achieved according to the statistical analysis of variance (ANOVA) for the most significant terms of the adsorption parameters and the interactions of the multi-variate combinations [22]. Thus, the Fischer test (F-test) and p-values (probability > F) was used to justify the significance of the terms involved. The higher F value and lower p-value (< 0.0500) are considered significant. The model p-values were less than 0.050 with F-values of 85.46 and 30.56 for NAP and PHE, respectively, implying the significance of the model. Thus, the

most significant terms for the NAP adsorption were A, B, C, AB, AC, and A2, while for PHE, A, B, AB and A^2 were of greater importance. Good agreement was established between the adjusted and predicted R^2 values with less than 20% differences for the NAP and PHE adsorption. Similarly, the model fitting can be analyzed based on the lack of fit test. In this case, the p-value for the lack of fit was greater than 0.05 with F-value of 0.59 and 1.70 for the NAP and PHE, respectively, thus, not significant relative to the pure error. The non-significant lack of fit is desirable for the model. The adequate precision for the model was greater than 4.00, precisely 28.2766 and 18.8869 for the NAP and PHE, respectively, indicating the adequacy and significance of the model.

The scatter plots have shown good agreement between the actual and predicted adsorption efficiency of the MOF as the all the values were not deviated from the perpendicular line as seen in Figure 1 and (c) for the NAP and PHE adsorption, respectively. Additionally, the studentized residual values (Figure 1 (b and d)) follows the normal distribution, suggesting the satisfaction of the adsorption data for the model.

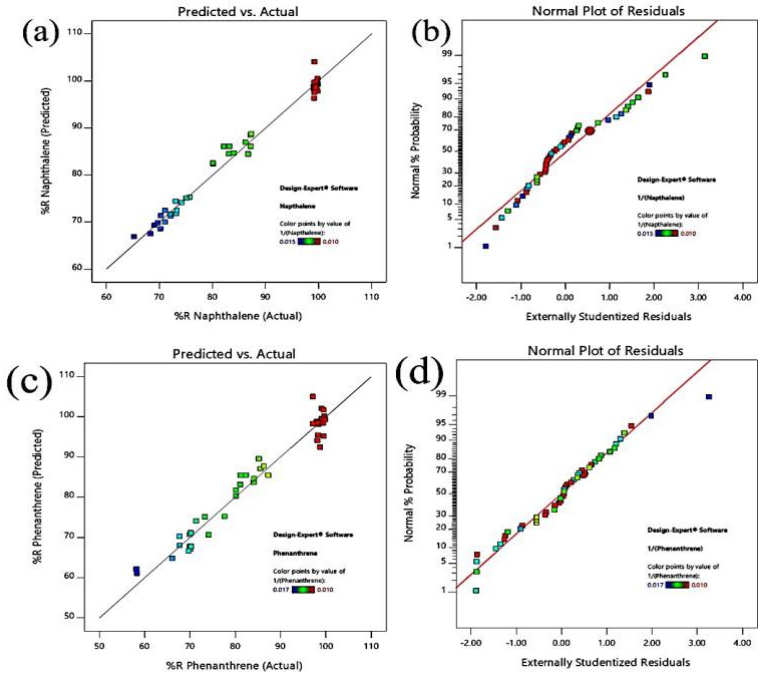

Figure 1. (a and c) Plot for the predicted vs actual values (b and d) normal probability plot for external studentized residuals for NAP and PHE adsorption onto NH_2-UiO-66(Zr).

3.2. ANN validation and predictions

The NAP and PHE adsorption onto NH_2-UiO-66(Zr) was described by the ANN model for the adsorption data comprising of 329 sets from the RSM optimizations. The fitting of the model analyzed according to the R^2 and RMSE values for the training, testing and validation data sets. The model training represented the model ability to learn the pattern of the data and the testing is used to make generalization of the ability of the network, while the validation is used to estimate the efficiency of the model [22]. Thus, the ANN architecture was obtained from the training data sets by varying the weight of the hidden neurons from 3-10, with the best fitting observed at node 6 with the highest R^2 of 0.999 and RMSE of 0.427 and 1.380 for NAP and PHE, respectively. Increasing the neurons weight above 6 resulted in a poor R2 and RMSE values. The ANN architecture was depicted in Figure 2 with the topography of 5-6-1 for both NAP and PHE.

The prediction of the ANN model for the NAP and PHE adsorption onto the NH_2-UiO-66(Zr) was also evaluated. The actual experimental adsorption efficiency of the MOFs based on the RSM conditions

were calculated and the ANN estimations were performed, and the values were highlighted in Table 1. The good prediction efficiency of the model was discovered based on the absolute errors calculated. The errors were in the range of 0.00 – 0.18 and 0.00 – 7.65% for the NAP and PHE, respectively, signifying the best fitting of the model for the former. Overall, the ANN possessed good potential for understanding the pattern of the data through the variable signals received from the hidden neurons [18] and make predictions of the output response with excellent efficiency.

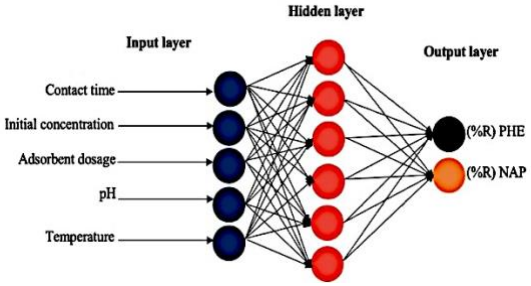

Figure 2. ANN architecture for NAP and PHE adsorption onto NH_2-UiO-66(Zr)

Table 1. ANN prediction for the competitive adsorption of NAP and PHE onto MIL-88(Fe).

						NAP removal (%R)			**PHE removal (%R)**		
Runs	Time	Dosage	Conc	pH	Temp	Actual	ANN predicted	Error	Actual	ANN predicted	Error
1	25	3	1	6	25	99.21	99.42	0.21	98.17	97.63	0.54
2	15	4	2	4	30	87.25	87.26	0.01	87.33	85.61	1.72
3	15	4	2	4	30	87.25	87.26	0.01	87.33	85.61	1.72
4	15	4	2	4	30	87.25	87.26	0.01	87.33	85.61	1.72
5	25	3	1	2	35	99.77	99.38	0.39	99.12	98.51	0.61
6	5	3	1	2	25	70.33	69.77	0.56	58.17	65.82	7.65
7	5	3	3	2	25	70.22	67.42	2.80	58.33	63.93	5.60
8	25	5	1	2	25	99.97	99.89	0.08	99.65	98.27	1.38
9	5	5	3	6	35	72.01	71.91	0.10	70.25	72.39	2.14
10	35	4	2	4	30	99.25	99.52	0.27	97.16	98.65	1.49
11	25	3	1	2	25	99.22	99.62	0.40	98.22	96.65	1.57
12	25	5	3	2	35	99.15	99.27	0.12	98.75	99.03	0.28
13	25	5	3	6	35	99.45	99.28	0.17	98.78	100.48	1.70
14	5	3	3	2	35	69.12	69.8	0.68	69.72	67.91	1.81
15	15	4	2	8	30	86.25	87.28	1.03	85.55	86.55	1.00
16	5	3	3	6	35	68.35	67.85	0.50	67.77	66.76	1.01
17	25	5	1	6	35	99.65	99.76	0.11	99.55	100.55	1.00
18	25	5	1	6	25	99.82	99.90	0.08	99.12	99.1	0.02
19	5	3	1	6	25	71.05	68.10	2.95	70.15	65.37	4.78
20	15	4	2	4	40	86.75	86.4	0.35	84.17	86.91	2.74
21	15	4	2	10	30	87.35	87.01	0.34	86.33	86.73	0.40
22	5	3	3	6	25	65.25	65.79	0.54	66.12	63.71	2.41
23	25	5	3	2	25	99.22	99.58	0.36	97.97	98.45	0.48
24	15	4	5	4	30	83.15	82.79	0.36	81.15	81.47	0.32
25	5	5	1	6	35	74.22	74.82	0.60	77.72	74.84	2.88
26	5	5	1	2	35	73.12	75.25	2.13	71.42	74.21	2.79
27	25	3	3	6	25	99.22	98.96	0.26	98.45	97.78	0.67
28	5	3	1	2	35	72.12	71.98	0.14	70.22	69.47	0.75
29	25	3	3	6	35	99.25	99.68	0.43	97.15	100.03	2.88
30	5	5	3	2	25	71.12	72.27	1.15	70.05	69.80	0.25
31	25	5	3	6	25	99.12	99.54	0.42	99.45	99.20	0.25

32	5	5	3	2	35	73.33	72.30	1.03	70.22	71.64	1.42
33	5	5	1	2	25	75.75	75.42	0.33	74.11	72.62	1.49
34	45	4	2	4	30	99.62	99.4	0.22	99.91	98.56	1.35
35	15	6	2	4	30	87.25	87.46	0.21	85.22	85.93	0.71
36	15	4	4	4	30	84.12	84.45	0.33	84.05	83.15	0.90
37	5	3	1	6	35	69.72	69.91	0.19	67.75	68.12	0.37
38	5	5	3	6	25	73.22	72.77	0.45	70.05	70.93	0.88
39	25	3	1	6	39	99.22	99.22	0.00	98.17	98.17	0.00
40	25	5	1	2	40	99.82	100.12	0.30	99.22	99.63	0.41
41	25	3	3	2	41	99.12	99.12	0.00	98.35	98.35	0.00
42	15	2	2	4	42	80.15	80.15	0.00	80.17	80.17	00.0
43	15	4	2	4	43	83.25	82.15	1.1	81.22	82.33	1.11
44	25	3	3	2	44	99.75	99.75	0.00	99.52	99.52	00.0
45	15	4	2	4	45	80.12	80.12	0.00	80.15	80.15	0.00
46	5	5	1	6	25	75.15	73.33	1.82	75.12	73.33	0.00
47	15	4	2	4	30	82.15	82.33	0.18	82.33	82.33	0.00

3.3. Reusability

Reusability studies has been one of the vital findings in adsorption [23]. Thus, adsorption study was performed with the regenerated MOF. The adsorption-desorption cycles were continuously repeated until 7 consecutive cycles as shown in Figure 3 (a), achieving higher removals. The adsorption efficiency was 89.1 and 87.2% for NAP and PHE respectively, at the 7th cycles, respectively. Tambat et al., previously reported on safranin adsorption onto regenerated NH2-UiO-66(Zr), achieving 93% adsorption efficiency within 3rd cycles [24]. Similarly, 87% adsorption of norfloxacin was reported at 5th cycle Fang et al [25]. The effective reusability of the MOF for pollutants adsorption was attributed to its higher porosity and stability in the aqueous medium [26, 27].

3.4. Binary adsorption of NAP and PHE

In real water samples, PAHs existed in a complex form, comprising a mixture of components. Thus, to ascertain the performance of the MOF for the effective PAHs remediation, competitive adsorption for the removal of NAP and PHE in a single medium. Effective adsorption of the pollutants was observed in the binary system with the adsorption efficiency of 97.7 and 96.9% for the NAP and PHE, respectively Figure 3(b). The higher efficiency for NAP adsorption was attributed to its lower molecular size as compared to the PHE. Their finding has shown that PHE achieved much lower adsorption capacity than the NAP, attributed to the competition of the pollutants for the active sites on the adsorbent. Overall, the good performance of the MOF was attributed to its porosity with BET surface area of 985 m^2/g, thus it provided sufficient adsorption sites for both NAP and PHE molecules.

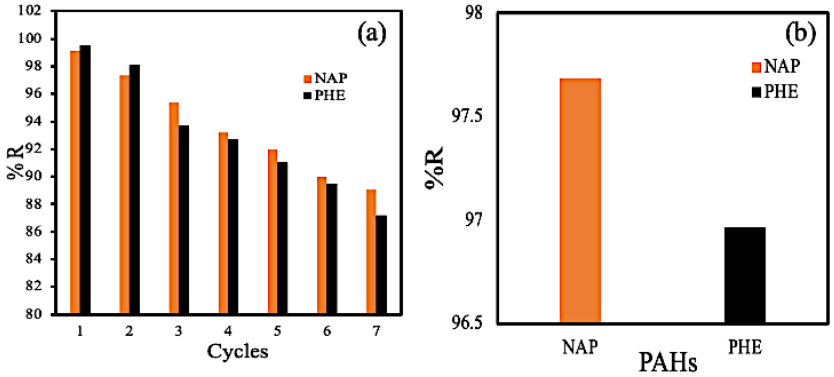

Figure 3. (a) Reusability and (b) binary adsorption of NAP and PHE onto NH_2-UiO-66(Zr).

4. Conclusions

Adsorption study was conducted for the removal of NAP and PHE onto NH_2-UiO-66(Zr) MOF. The process was optimized by RSM, and the model fitting was significant for the PAHs with overall p-value less than 0.05 and the F-values of 85.46 and 30.56 for NAP and PHE, respectively. Similarly, the consistency of the model was described by good agreements between the adjusted and predicted R^2 with less than 20 % differences. The adequate precision of the model was 28.2766 and 18.8869 for the NAP and PHE, respectively, confirming the adequacy of the model with lower signal to noise ratio. Thus, the RSM model was validated by ANN analysis using multi-layer perceptron with backward propagation and the best architecture was obtained at node 6. The reusability of the MOF for the pollutant's adsorption was also studied recording up to 7 cycles performance with the adsorption efficiency of 89.1 and 87.2 % for the NAP and PHE, respectively. The good performance of the MOF was also studied in binary system, and the adsorption efficiency achieved was 97.7 and 96.9 % for the NAP and PHE, respectively, confirming the efficiency of the MOF for the PAHs adsorption and could be employed for real sample applications.

Acknowledgement

We would like to acknowledge FGRS grant received from Ministry of Higher Education (MOHE) with cost center number FRGS/1/2020/STG04/UTP/02/3 and YUTP grant (015LCO-283).

References

[1] Zhang Y, Zhang L, Huang Z, Li Y, Li J, Wu N, He J, Zhang Z, Liu Y and Niu Z 2019 Pollution of polycyclic aromatic hydrocarbons (PAHs) in drinking water of China: Composition, distribution and influencing factors *Ecotoxicol. Environ. Saf.* **177** 108–16.

[2] Honda M and Suzuki N 2020 Toxicities of Polycyclic Aromatic Hydrocarbons for Aquatic Animals *Int. J. Environ. Res. Public Health* **17** 1363.

[3] Gupta H and Singh S 2018 Kinetics and thermodynamics of phenanthrene adsorption from water on orange rind activated carbon *Environ. Technol. Innov.* **10** 208–14.

[4] Rabodonirina S, Net S, Ouddane B, Merhaby D, Dumoulin D, Popescu T and Ravelonandro P 2015 Distribution of persistent organic pollutants (PAHs, Me-PAHs, PCBs) in dissolved, particulate and sedimentary phases in freshwater systems *Environ. Pollut.* **206** 38–48.

[5] Ye X, Pan W, Li C, Ma X, Yin S, Zhou J and Liu J 2020 Exposure to polycyclic aromatic hydrocarbons and risk for premature ovarian failure and reproductive hormones imbalance *J. Environ. Sci. (China)* **91** 1–9.

[6] Cabal B, Budinova T, Ania C O, Tsyntsarski B, Parra J B and Petrova B 2009 Adsorption of naphthalene from aqueous solution on activated carbons obtained from bean pods *J. Hazard. Mater.* **161** 1150–6.

[7] Ania C O, Cabal B, Parra J B and Pis J J 2007 Importance of the hydrophobic character of activated carbons on the removal of naphthalene from the aqueous phase *Adsorpt. Sci. Technol.* **25** 155–67.

[8] Goswami L, Kumar R V, Manikandan N A, Pakshirajan K and Pugazhenthi G 2017 Simultaneous polycyclic aromatic hydrocarbon degradation and lipid accumulation by Rhodococcus opacus for potential biodiesel production *J. Water Process Eng.* **17** 1–10.

[9] Sponza D T and Oztekin R 2010 Removals of PAHs and acute toxicity via sonication in a petrochemical industry wastewater *Chem. Eng. J.* **162** 142–50.

[10] Zango Z U, Sambudi N S, Jumbri K, Ramli A, Hana N, Abu H, Saad B, Nur M, Rozaini H, Isiyaka H A, Osman A M and Sulieman A 2020 An Overview and Evaluation of Highly Porous Adsorbent Materials for Polycyclic Aromatic Hydrocarbons and Phenols Removal from Wastewater *Water* **12**(10) 1–40.

[11] Ania C O, Cabal B, Pevida C, Arenillas A, Parra J B, Rubiera F and Pis J J 2007 Removal of naphthalene from aqueous solution on chemically modified activated carbons *Water Res.* **41** 333–40.

[12] Zango Z U, Jumbri K, Sambudi N S, Ramli A, Bakar N H H A, Saad B, Rozaini M N H, Isiyaka H A, Jagaba A H, Aldaghri O and Sulieman A 2020 A critical review on metal-organic frameworks and their composites as advanced materials for adsorption and photocatalytic degradation of emerging organic pollutants from wastewater *Polymers (Basel).* **12** 1–42.
[13] Zha Q, Sang X, Liu D, Wang D, Shi G and Ni C 2019 Modification of hydrophilic amine-functionalized metal-organic frameworks to hydrophobic for dye adsorption *J. Solid State Chem.* **275** 23–9.
[14] Zou D and Liu D 2019 Understanding the modifications and applications of highly stable porous frameworks via UiO-66 *Mater. Today Chem.* **12** 139–65.
[15] Zango Z U, Abu Bakar N H H, Sambudi N S, Jumbri K, Abdullah N A F, Abdul Kadir E and Saad B 2019 Adsorption of chrysene in aqueous solution onto MIL-88(Fe) and NH_2-MIL-88(Fe) metal-organic frameworks: kinetics, isotherms, thermodynamics and docking simulation studies *J. Environ. Chem. Eng.*.
[16] Zango Z U, Jumbri K, Sambudi N S, Abu Bakar N H H, Abdullah N A F, Basheer C and Saad B 2019 Removal of anthracene in water by MIL-88(Fe), NH2-MIL-88(Fe), and mixed-MIL-88(Fe) metal–organic frameworks *RCS Adv.* **9** 41490–501.
[17] Afolabi I C, Popoola S I and Bello O S 2020 Machine learning approach for prediction of paracetamol adsorption efficiency on chemically modified orange peel *Spectrochim. Acta - Part A Mol. Biomol. Spectrosc.* **243** 118769.
[18] Messikh N, Bousba S and Bougdah N 2017 The use of a multilayer perceptron (MLP) for modelling the phenol removal by emulsion liquid membrane *J. Environ. Chem. Eng.* **5** 3483–9.
[19] Zango Z U, Ramli A, Jumbri K, Soraya N, Ahmad H I, Hana N, Abu H and Saad B 2020 Optimization studies and artificial neural network modeling for pyrene adsorption onto UiO-66(Zr) and NH_2-UiO-66(Zr) metal organic frameworks *Polyhedron* **192** 114857.
[20] Isiyaka H A, Jumbri K, Sambudi N S, Zango Z U, Fathihah Abdullah N A, Saad B and Mustapha A 2020 Adsorption of dicamba and MCPA onto MIL-53(Al) metal-organic framework: Response surface methodology and artificial neural network model studies *RSC Adv.* **10** 43213–24.
[21] Zango Z U, Sambudi N S, Jumbri K, Abu Bakar N H H, Abdullah N A F, Negim E S M and Saad B 2020 Experimental and molecular docking model studies for the adsorption of polycyclic aromatic hydrocarbons onto UiO-66(Zr) and NH_2-UiO-66(Zr) metal-organic frameworks *Chem. Eng. Sci.* **220** 1–12.
[22] Isiyaka H A, Jumbri K, Sambudi N S, Lim J W, Saad B, Ramli A and Zango Z U 2021 Experimental and Modeling of Dicamba Adsorption in Aqueous Medium Using MIL-101(Cr) Metal-Organic Framework *Processes* **9** 1–18.
[23] Zango Z U, Sambudi N S, Jumbri K, Abu Bakar N H H and Saad B 2020 Removal of Pyrene from Aqueous Solution Using Fe-based Metal-organic Frameworks *IOP Conf. Ser. Earth Environ. Sci.* **549** 012061.
[24] Tambat S N, Sane P K, Suresh S, Varadan O. N, Pandit A B and Sontakke S M 2018 Hydrothermal synthesis of NH_2-UiO-66 and its application for adsorptive removal of dye *Adv. Powder Technol.* **29** 2626–32.
[25] Fang X, Wu S, Wu Y, Yang W, Li Y, He J, Hong P, Nie M, Xie C, Wu Z, Zhang K, Kong L and Liu J 2020 High-efficiency adsorption of norfloxacin using octahedral UIO-66-NH_2 nanomaterials: Dynamics, thermodynamics, and mechanisms *Appl. Surf. Sci.* **518**.
[26] Yang Z, Zhu L and Chen L 2019 Selective adsorption and separation of dyes from aqueous solution by core-shell structured NH2-functionalized UiO-66 magnetic composites *J. Colloid Interface Sci.* **539** 76–86.
[27] Chen Q, He Q, Lv M, Xu Y, Yang H, Liu X and Wei F 2015 Selective adsorption of cationic dyes by UiO-66-NH_2 *Appl. Surf. Sci.* **327** 77–85.